A Vestige of Earth's Oldest Ophiolite

Harald Furnes, *et al.*

Science **315**, 1704 (2007);
DOI: 10.1126/science.1139170

Science (print ISSN 0036-8075; online ISSN 1095-9203) is published weekly, except the last week in December, by the American Association for the Advancement of Science, 1200 New York Avenue NW, Washington, DC 20005.

25. U. Wyputta, B. J. McAvaney, *Clim. Dyn.* **17**, 923 (2001).
26. G. Ramstein, Y. Serafini-Le Treut, H. Le Treut, M. Forichon, S. Joussaume, *Clim. Dyn.* **14**, 233 (1998).
27. T. Blunier *et al.*, *Geophys. Res. Lett.* **24**, 2683 (1997).
28. P. Camberlin, S. Janicot, I. Poccard, *Int. J. Climatol.* **21**, 973 (2001).
29. D. W. Johnson, P. J. Hanson, D. E. Todd, R. B. Susfalk, C. F. Trettin, *Water Air Soil Pollut.* **105**, 251 (1998).
30. C. J. Willmott, S. M. Robeson, *Int. J. Climatol.* **15**, 221 (1995).
31. M. Stuiver, P. M. Grootes, *Quat. Res.* **53**, 277 (2000).
32. We thank R. R. Schneider for providing samples from core GeoB 6518-1 and E. C. Hopmans for analytical support with the high-performance liquid chromatography/mass spectrometry instrument. This research was supported by the Earth and Life Sciences Council of the Netherlands Organization for Scientific Research and the Deutsche Forschungsgemeinschaft.

Supporting Online Material
www.sciencemag.org/cgi/content/full/315/5819/1701/DC1
Materials and Methods
SOM Text
Figs. S1 and S2
References

29 November 2006; accepted 22 February 2007
10.1126/science.1138131

A Vestige of Earth's Oldest Ophiolite

Harald Furnes,[1]* Maarten de Wit,[2,3] Hubert Staudigel,[4] Minik Rosing,[5] Karlis Muehlenbachs[6]

A sheeted-dike complex within the ~3.8-billion-year-old Isua supracrustal belt (ISB) in southwest Greenland provides the oldest evidence of oceanic crustal accretion by spreading. The geochemistry of the dikes and associated pillow lavas demonstrates an intraoceanic island arc and mid-ocean ridge–like setting, and their oxygen isotopes suggest a hydrothermal ocean-floor–type metamorphism. The pillows and dikes are associated with gabbroic and ultramafic rocks that together make up an ophiolitic association: the Paleoarchean Isua ophiolite complex. These sheeted dikes offer evidence for remnants of oceanic crust formed by sea-floor spreading of the earliest intact rocks on Earth.

Ophiolites represent sections of oceanic crust that were generated by sea-floor spreading and later emplaced onto continental margins (*1*). Originally, ophiolites were assumed to represent oceanic crust formed at mid-ocean ridges, but this view has changed radically, and it is becoming clear that the majority of ophiolites are generated in supra–subduction-zone environments (*1*). Depending on their tectonic environment of formation and their structural architecture and geochemical affinities, Phanerozoic ophiolites can be classified into different types, but the majority are genetically related to subduction environments (*1*, *2*). A complete ophiolite consists of submarine basaltic volcanic rocks (mainly pillow lavas), sheeted dikes, a plutonic complex, and upper-mantle rocks. However, many ophiolites lack one or more of these components (*2*). In Archean greenstone belts, the absence of complete ophiolite pseudostratigraphies (in particular, sheeted dikes and gabbros) has led many workers to conclude that ophiolites are not represented in the earliest stages of Earth's history (*3*–*5*). The oldest purported example is the 2505-million-year-old Dongwanzi ophiolite complex in the North China craton (*6*), which is a disputed claim (*7*).

It has been suggested that several Archean greenstone belts host dismembered ophiolites (*8*, *9*). Nonetheless, the question of whether Archaean oceanic crust formed by sea-floor spreading was related to Phanerozoic-like plate tectonics has so far remained conjectural because of the absence of compelling kinematic evidence to discriminate between origins through the horizontal motion of plates at divergent plate boundaries or through vertical motion above mantle plumes. Sheeted dikes provide an answer to these questions because they form by sea-floor spreading and accretion during horizontal movement at divergent plate boundaries, and they are considered to be crucial components of ophiolites. Here we report the discovery of a sheeted-dike complex within the Paleoarchean Isua supracrustal belt (ISB). This and the associated rocks, together with their compositions, make up a ~3.8-billion-year-old ophiolite, which in turn has strong

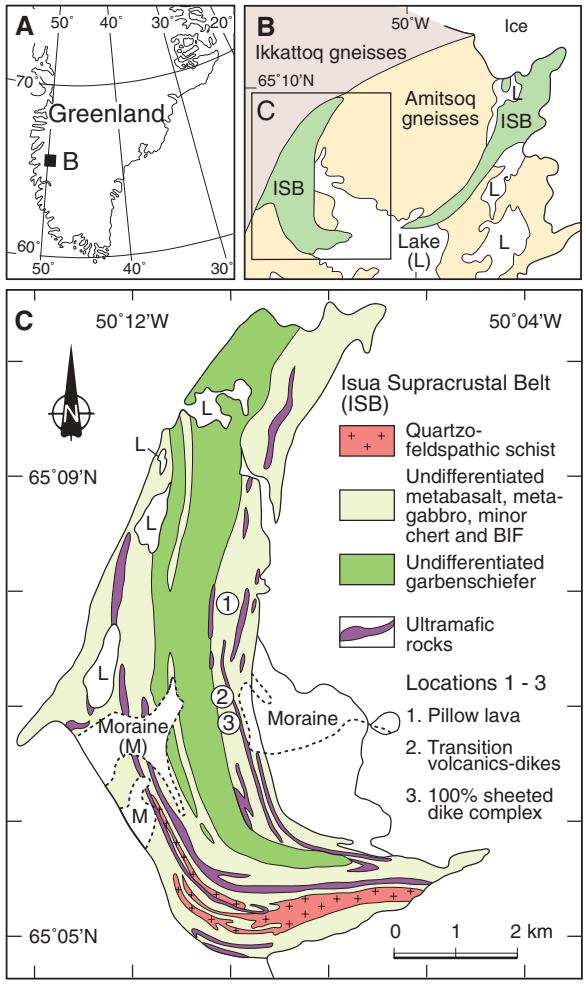

Fig. 1. (**A**) Location of the ISB in southwestern Greenland. The black square shows the location of the area detailed in (B). (**B**) ISB and adjacent gneisses. (Inset) Location of the area detailed in (C). (**C**) Simplified geological map of the western arm of the ISB, showing locations (1 to 3) of the 100% sheeted-dike complex (3: latitude 65.05.335°N, longitude 50.10.661°W) grading into dikes and volcanic rocks (2: latitude 65.07.033°N, longitude 50.09.769°W) and volcanic rocks (1: latitude 65.07.889°N, longitude 50.09.835°W). The geological maps [(**B**) and (C)] are modified from (*10*, *13*, *15*).

[1]Centre for Geobiology and Department of Earth Science, University of Bergen, Bergen, Norway. [2]Africa Earth Observatory Network (AEON) and Department of Geological Sciences, University of Cape Town, Rondebosch 7700 South Africa. [3]GeoForschungsZentrum (GFZ)–Potsdam, Telegraphenberg, Potsdam, Germany. [4]Scripps Institution of Oceanography, University of California, San Diego, La Jolla, CA 92093-0225, USA. [5]Nordic Centre for Earth Evolution and Geological Museum, University of Copenhagen, 1350, København K, Denmark [6]Department of Earth and Atmospheric Sciences, University of Alberta, Edmonton, Alberta T6G 2E3, Canada.

*To whom correspondence should be addressed. E-mail: harald.furnes@geo.uib.no

implications about the early tectonic and geochemical evolution of Earth.

The ISB, situated in southwestern Greenland (Fig. 1A), defines an arcuate belt ~35 km long and 2.5 km thick (Fig. 1B) that contains a variety of igneous and sedimentary rocks (*10*, *11*). In general, the rocks are strongly deformed and metamorphosed to amphibolite facies, and primary features are scarce. The main lithologies of the ISB are metabasalts (amphibolites), metagabbros and ultramafics associated with metapelites, cherts, banded iron formations (BIFs), and felsic rocks (*11*), now preserved as enclaves within the surrounding plutons (Ikkattoq and Amitsoq gneisses) (Fig. 1B).

Pillow structures and associated hyaloclastites are common within the amphibolites (*12*, *13*) and provide unequivocal evidence of submarine lavas. Another major component (~50%) of the ISB, a unit described as "garbenschiefer," was first considered to be derived from mafic intrusions (*10*), but has been reinterpreted as a volcano sedimentary sequence containing gabbro sills (*11*, *13*, *14*). It has been suggested that together these assemblages represent oceanic-like crust that may have been obducted within an accretionary wedge ~3.7 billion years ago, as a result of plate tectonic–like processes (*12*).

Radiometric dating (U/Pb and Pb/Pb) has shown that the ISB formed between ~3800 and 3700 million years ago (Ma) (*14*). Whole-rock Sm-Nd isochrons define ages of 3779 ± 81 Ma from metasediments and enclosing garbenschiefer (*15*) and 3777 ± 44 Ma from pillow lavas and metagabbro (*16*). The latter date is partly based on samples collected from location 1 of this study (Fig. 1C).

We examined a number of sections in the eastern part of the western arm of the ISB, mapped as variegated schists (*10*) and amphibolites (*13*, *17*) within the area around locations 1 to 3 (Fig. 1C). Location 1 shows well-preserved metabasaltic pillow lava (Fig. 2A), in places with small triangular pockets of interpillow hyaloclastite (Fig. 2A). Locally, the pillows contain felsic ocelli (Fig. 2B) and rare amygdales. The rocks are homogeneously deformed and contain a cleavage that is subparallel to the lithological layering. Deformed ocelli (originally spherical) indicate deformation with 80 to 90% shortening perpendicular to the cleavage and 200 to 250% extension along a well-defined lineation plunging 72°S. At location 2, ~1.5 km south of location 1 (Fig. 1C), the sequence consists of tabular subparallel dikes with intervening centimeter- to decimeter-thick zones of lenticular-to-irregular screens of volcanic material (Fig. 2, C and D, and fig. S1), and locally, plagiogranite occurs [Fig. 2D and supporting online material (SOM)]. Approximately 500 m further south, at location 3, the mixed dike/volcanic sequence changes structurally downward into a sheeted complex consisting of 100% tabular dikes (Fig. 2E and fig. S2), which to the west is in tectonic contact with metagabbro and ultramafic sheets. Individual dikes range in width from 2 to 50 cm. Dikes have both one- and (mostly) two-way fine-grained chilled planar margins (Fig. 2E). Cross-cutting dikes are also observed (Fig. 2F). We examined a number of sections across a 30–to–50-m-wide subvertical sequence of dikes, which we interpret as part of a sheeted-dike complex with an estimated predeformation width of >200 m.

Petrographically, the central parts of the dikes consist of fine-grained (~300 μm) plagioclase, amphibole (predominant), and biotite with relic subophitic texture (Fig. 2G). The dark green (commonly schistose) marginal zones, inferred to represent chilled margins (Fig. 2E), consist of dense (~100 μm) monomineralic zones of amphibole (Fig. 2H). These chilled margins of the dikes are texturally and mineralogically similar to the margins of the pillows.

Mafic gneisses interpreted as metagabbros occur as scattered outcrops within an area of ~100 by 100 m in the southwestern part of the ISB. They are uniform amphibolites characterized by centimeter-scale discontinuous layers and lenses of plagioclase in a hornblende-quartz-plagioclase matrix (fig. S3), representing a highly deformed and metamorphosed gabbroic texture. This contrasts with most Isua amphibolites, which typically consist of lithological units <1 m across strike (Fig. 2, C and D). Felsic dikes of the Amitsoq gneisses crosscut the metagabbros and define the early Archean age of the Isua supracrustals.

The ultramafic rocks (fig. S4), which occur mainly along the boundaries of the western belt of the ISB, have been variably transformed to serpentinites and calc-silicate rocks by metasomatic processes (*11*). These layered meta-ultramafic rocks are associated with the sheeted-dike complex (Fig. 1C) and metagabbro, sometimes with uninterrupted transitions from layered ultramafic sequence into gabbros (*18*).

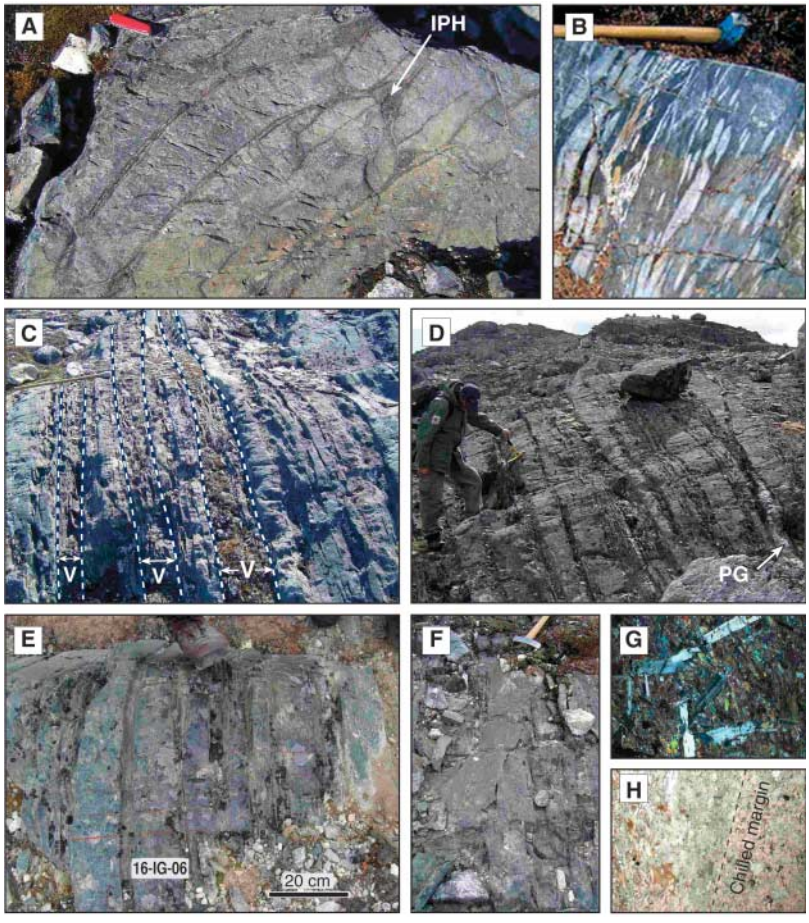

Fig. 2. (**A**) Well-preserved pillow lava exhibiting chilled margins (dark selvages) and pockets of interpillow hyaloclastite (IPH). (**B**) Ocelli-bearing pillows. The pale gray ocelli, originally spheres, give a measure of the deformation that the rocks have suffered. (A) and (B) are from location 1. (**C**) Dikes with intervening layers of volcanic rocks (V). (**D**) Nearly 100% sheeted dikes with minor amounts of interdike volcanic material. Dikes can be traced along strike for more than 20 m. The white lens (bottom right) is a plagiogranite (PG). (C) and (D) are from location 2. (**E**) 100% sheeted-dike complex. The weathered-out zones are amphibole schist, originally chilled margins. (**F**) Two crosscutting layers (just below the hammer head). (E) and (F) are from location 3. [(**G**) and (**H**)] Photomicrographs of the central part of the dike (G), showing relict subophitic texture (plane-polarized light image), and chilled margin of the dike (H), consisting predominantly of fine-grained amphibole (plane light image).

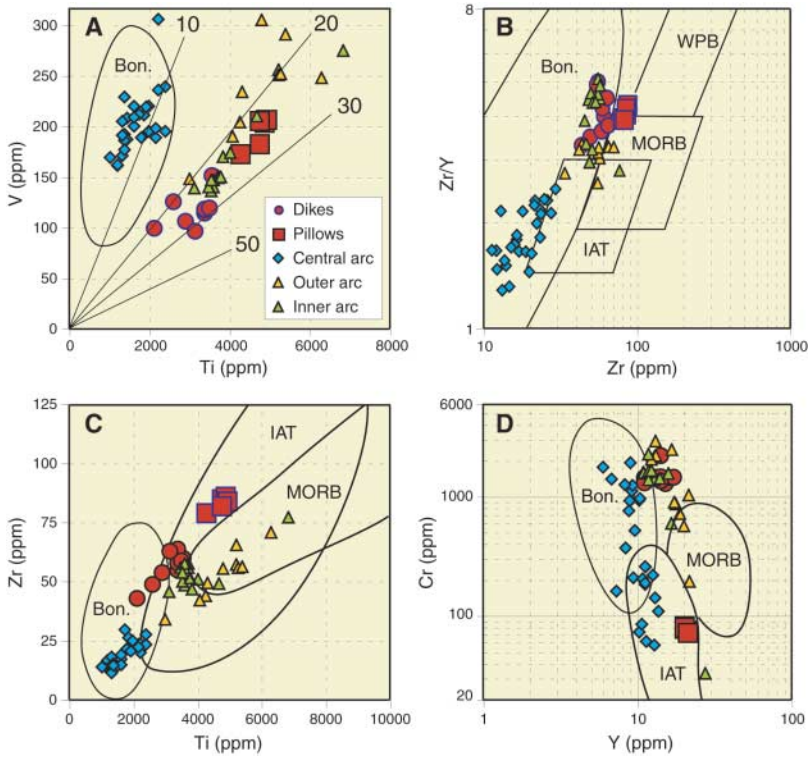

Fig. 3. (**A**) Ti-V, (**B**) Zr-Zr/Y, (**C**) Ti-Zr, and (**D**) Y-Cr discrimination diagrams (*1*). The geochemical data from the central-, outer-, and inner-arc tectonic domains (undifferentiated metabasalts) are from (*17*, *19*). The new geochemical data of this study are shown in red. The boninite data are from (*21*). The Ti/V ratios in (A) are characteristic of the following: 10 to 20, island arc; 20 to 50, MORB; 20 to 30, mixed MORB and island arc; and 10 to 50, back-arc basins. Bon, boninites; IAT, island-arc tholeiite; and WPB, within-plate basalt.

Table 1. Summary of $\delta^{18}O$ results.

Sample	Type	$\delta^{18}O$ (standard mean ocean water)*
03-3.5	Pillow core	9.9
03-3.13	Pillow core	6.8
03-3.22	Pillow core	7.3
03-3.23	Pillow core	6.9
03-3.31	Pillow core	6.7
03-3.39	Pillow core	6.5
03-3.40	Pillow core	6.6
1A2-IG-06	Pillow core	6.8
1B4-IG-06	Pillow core	6.8
2A-IG-06	Pillow core	6.9
2B2A-IG-06	Pillow core	7.1
3A2A-IG-06	Pillow core	6.8
5B1-IG-06	Pillow core	7.9
5C-IG-06	Pillow core	7.6
6B-IG-06	Pillow core	6.8
7-IG-06	Dike	5.9
8-IG-06	Dike	6.0
9-IG-06	Dike	6.1
16A-IG-06	Dike	6.0
16C-IG-06	Dike	6.3
16E-IG-06	Dike	6.9
16G-IG-06	Dike	6.9
17A-IG-06	Dike	5.8
17B-IG-06	Dike	5.7

*See SOM.

The geochemistry of pillow lava and dikes from locations 1 and 3 (Fig. 1C), as well as that of the least altered samples of previous studies (*17*, *19*), has been plotted in discriminant diagrams with various combinations of the relatively immobile elements Ti, V, Cr, Y, and Zr (*1*). The new geochemical data (table S1 and SOM) demonstrate intraoceanic island arc and mid-ocean ridge basalt (MORB) affinities (Fig. 3), as previously concluded (*19*). Furthermore, the similarities in the concentrations of incompatible elements (Ti, V, Zr, and Y) and their ratios (Zr/Y) strongly suggest that the pillow lavas and the dikes are cogenetic, supporting our field observations regarding their spatial and temporal relationships. It has been demonstrated that the metabasalts of the central garbenschiefer unit are geochemically similar to boninites (*17*) (Fig. 3). The presence of boninites is important in the evaluation of the tectonic environment, because they are generally associated with modern intraoceanic island arcs and are thought to be related to proto-arc and back-arc spreading (*20*–*22*). This magmatic progression suggests that ophiolites are geochemically heterogeneous and that their tectonic evolution may have involved initial sea-floor spreading, followed by subduction initiation and one or more episodes of arc splitting and basin opening (*20*, *21*).

Oxygen isotope data from locations 1 and 3 (Fig. 1C) show that the pillows are more enriched in ^{18}O than the dikes (Table 1 and SOM). Although the $\delta^{18}O$ values of the central part of the pillows range between 6.5 and 9.9 (average, 7.2), the dikes show a narrower range between 5.7 and 6.9 (average, 6.3). These rocks do not record primary magmatic oxygen isotope values but may record alteration by 0 to +2 of the $\delta^{18}O$ value of seawater at a spreading ridge. The pillows are more enriched in ^{18}O because they altered at lower temperatures than did the dikes, and oxygen isotope fractionation decreases in magnitude with increasing temperature (*23*). Collectively, these data and the relic subophitic textures in the sheeted dikes are consistent with the seawater/rock interaction during ocean-floor metamorphism that takes place at modern spreading ridges (SOM) and which has been documented in most ophiolites of Phanerozoic and Proterozoic ages (*24*, *25*). This finding is also consistent with fluid-inclusion studies on amygdales in the ISB pillow breccias that indicate alteration during early sea-floor–like hydrothermal metamorphism (*26*).

We provide three robust lines of evidence for an Isua ophiolite complex as a vestige of Archean supra–subduction-zone oceanic crust. First, the sheeted-dike complex and cogenetic pillow lavas represent the upper-crustal section of a dismembered ophiolite. The sheeted-dike complex provides compelling structural evidence of horizontal extension by dike injection at a spreading ridge (SOM). Second, we reject the scenario of dike injection above a plume head in a non–plate tectonic environment, given the oceanic island arc and MORB geochemical characteristics of the pillow lavas and dikes reported here, together with the data from (*19*). Further, the boninitic affinity of the central garbenschiefer (*17*) is similar to that of Phanerozoic supra–subduction-zone ophiolites with a protracted tectonomagmatic evolution history (*20*, *22*). Third, the oxygen isotope compositions of the pillow lavas and dikes and their petrographic textures are compatible with sea-floor hydrothermal metamorphism at a spreading ridge. Although the strain history of these rocks is not yet sufficiently well known to permit a detailed reconstruction of the Isua ophiolite complex, we contend that the ISB preserves vestiges of Earth's oldest ophiolite and oceanic crust. This implies that sea-floor spreading and subduction processes of Phanerozoic-like plate tectonics were operating ~3.8 billion years ago, as proposed by Komiya *et al*. (*12*).

References and Notes

1. J. A. Pearce, *Geol. Soc. Am. Spec. Pap. 373* (2003), p. 269.
2. Y. Dilek, *Geol. Soc. Am. Spec. Pap. 373* (2003), p. 1.
3. M. J. Bickle, E. G. Nisbet, A. Martin, *J. Geol.* **102**, 121 (1994).
4. W. B. Hamilton, *Geol. Soc. Am. Today* **13**, 4 (2003).

5. R. J. Stern, *Geology* **33**, 557 (2005).
6. T. M. Kusky, J.-H. Li, R. D. Tucker, *Science* **292**, 1142 (2001).
7. M. Zhai, G. Zhao, Q. Zhang, *Science* **295**, 923a (2002).
8. T. M. Kusky, Ed., *Precambrian Ophiolites and Related Rocks* (Elsevier, Amsterdam, 2004).
9. M. J. de Wit, in *Developments in Precambrian Geology,* vol. 13, T. M. Kusky, Ed. (Elsevier, London, 2004), pp. 599–614.
10. A. P. Nutman, *Greenland Geol. Surv.* Bulletin 154 (1986).
11. M. T. Rosing, N. M. Rose, D. Bridgwater, H. S. Thomsen, *Geology* **24**, 43 (1996).
12. T. Komiya *et al.*, *J. Geol.* **107**, 515 (1999).
13. J. S. Myers, *Precambrian Res.* **105**, 129 (2001).
14. A. P. Nutman, V. C. Bennett, C. R. L. Friend, M. T. Rosing, *Chem. Geol.* **141**, 271 (1997).
15. M. T. Rosing, *Science* **283**, 674 (1999).
16. M. Boyet *et al.*, *Earth Planet. Sci. Lett.* **214**, 427 (2003).
17. A. Polat, A. W. Hofmann, M. T. Rosing, *Chem. Geol.* **184**, 231 (2002).
18. A. P. Nutman, V. R. McGregor, C. R. L. Friend, V. C. Bennet, P. D. Kinny, *Precambrian Res.* **78**, 1 (1996).
19. A. Polat, A. W. Hofmann, *Precambrian Res.* **126**, 197 (2003).
20. Y. Dilek, M. J. F. Flower, *Geol. Soc. London Spec. Publ.* **218**, 43 (2003).
21. A. J. Crawford, Ed., *Boninites* (Unwin Hyman, London, 1989).
22. R. B. Pedersen, H. Furnes, *J. Geodyn.* **13**, 183 (1991).
23. K. Muehlenbachs, *Chem. Geol.* **145**, 263 (1998).
24. D. S. Stakes, H. P. Taylor Jr., *J. Geophys. Res.* **97**, 7043 (1992).
25. C. Holmden, K. Muehlenbachs, *Science* **259**, 1733 (1993).
26. J. L. R. Touret, *Precambrian Res.* **126**, 219 (2003).

27. Comments by Y. Dilek, B. Robins, N. McLoughlin, and two anonymous reviewers improved the manuscript. Financial support was provided by the Norwegian Research Council, the Geological Museum of Copenhagen, the GFZ-Potsdam, the Agouron foundation, and the National Sciences and Engineering Research Council of Canada. This is AEON contribution no. 31.

Supporting Online Material

www.sciencemag.org/cgi/content/full/315/5819/1704/DC1
SOM Text
Figs. S1 to S4
Table S1
References

21 December 2006; accepted 7 February 2007
10.1126/science.1139170

Bottom-Up Determination of Air-Sea Momentum Exchange Under a Major Tropical Cyclone

Ewa Jarosz,* Douglas A. Mitchell,† David W. Wang, William J. Teague

As a result of increasing frequency and intensity of tropical cyclones, an accurate forecasting of cyclone evolution and ocean response is becoming even more important to reduce threats to lives and property in coastal regions. To improve predictions, accurate evaluation of the air-sea momentum exchange is required. Using current observations recorded during a major tropical cyclone, we have estimated this momentum transfer from the ocean side of the air-sea interface, and we discuss it in terms of the drag coefficient. For winds between 20 and 48 meters per second, this coefficient initially increases and peaks at winds of about 32 meters per second before decreasing.

The air-sea momentum exchange under a tropical cyclone determines the oceanic response to its winds. An accurate estimation of the exchange hence is required for correctly forecasting storm track and intensity, as well as for accurately predicting storm surges, ocean currents, and waves, and for making hurricane risk assessments, particularly because the frequency and intensity of tropical cyclones are reportedly increasing (*1*). Conventional methods of determining the air-sea momentum transfer are from the atmospheric side of the interface and are based on measurements of wind profiles near the ocean surface or of wind turbulence (*2*). These methods, however, cannot work reliably for the extreme high-wind conditions of a major tropical cyclone, because wind measurements near the ocean interface are inevitably contaminated from intense breaking-wave activities and sea spray (*3*).

Most available field measurements of surface stress are for wind speeds ranging from 4 to 20 m s^{-1}. The techniques employed estimate the interface momentum exchange as a wind stress, τ_s, given by

$$\tau_s = \rho_{air} C_D |\mathbf{W}|^2 \quad (1)$$

where ρ_{air} is the air density, C_D is the drag coefficient, and $|\mathbf{W}|$ is the velocity magnitude of the wind at a reference height (usually 10 m).

In open ocean conditions, as the wind becomes stronger the range of surface waves, which travel at slower speeds than the wind, widens. Accordingly, C_D increases as wind speed increases (*3*). This pattern of variability in C_D is commonly used in wave, surge, and circulation numerical models, which incorporate a monotonic increase of the drag coefficient with wind speed even under extreme wind conditions. Such an assumption may result in an overestimation of the air-sea momentum transfer and lead to unrealistic model predictions or, perhaps even worse, model tuning using bad physical justifications.

Recently, limited meteorological observations, theory, and experiments (*3*–*8*) suggest a reduction in the drag coefficient at high wind speeds, generally greater than 30 m s^{-1}. All these efforts to evaluate the air-sea momentum exchange have been made through meteorological measurements, or theories and models developed for the atmospheric boundary layer ("top-down" determination). Estimation of this exchange can also be done from the other side of the interface with full water-column ocean current observations. This method directly determines the stress at the interface based on ocean currents and provides a very reliable and accurate direct determination of the air-sea momentum transfer under high winds (*3*). However, this type of "bottom-up" determination imposes the almost impossible requirements of deploying instruments in the ocean directly under the highly unpredictable path of a major tropical cyclone and then having the instruments survive the enormous forces generated by the cyclone.

On 15 September 2004, the center of Hurricane Ivan (at category 4 strength) passed directly over six current and wave/tide gauge moorings on the outer continental shelf in the northeastern Gulf of Mexico (*9*–*12*) (Fig. 1). The instrumentation survived and measured nearly full ocean current velocity profiles directly under the cyclone. The resulting data set allows direct "bottom-up" determination of the air-sea momentum exchange under extreme wind conditions.

Extreme winds of a tropical cyclone elicit a four-stage response when passing over ocean waters (*9*, *13*). The first three stages make up the "forced stage" response, whereas the fourth stage is the "relaxation stage." Over the open ocean, the forced stage response is primarily baroclinic (depth-dependent), with a weak barotropic (depth-independent) response consisting of a trough in sea surface height and an associated geostrophic current that are set up almost instantly (*13*). Over the continental shelf, however, the forced response is quite different (*9*). It consists of a strong barotropic component that is not geostrophically balanced and a much weaker baroclinic response. Thus, the directly forced response on the continental shelf should be well described to the first order by the linear time-dependent depth-integrated horizontal momentum equations. Scaling analysis of current velocity measurements recorded in the northeastern Gulf of Mexico (Fig. 1) under Hurricane Ivan supports this assumption, especially for the along-

Naval Research Laboratory, Stennis Space Center, MS 39529–5004, USA.

*To whom correspondence should be addressed. E-mail: ewa.jarosz@nrlssc.navy.mil
†Present address: Exxon Mobil Upstream Research Company, Houston, TX 77027–6019, USA.